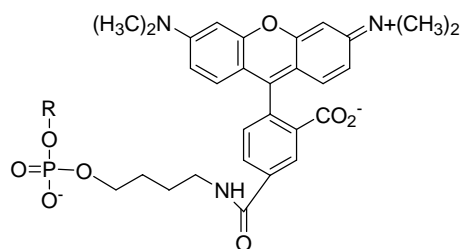
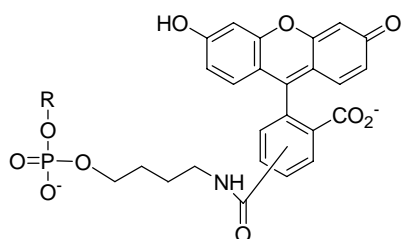


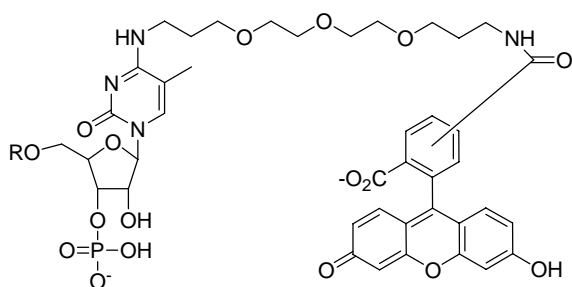
**a**

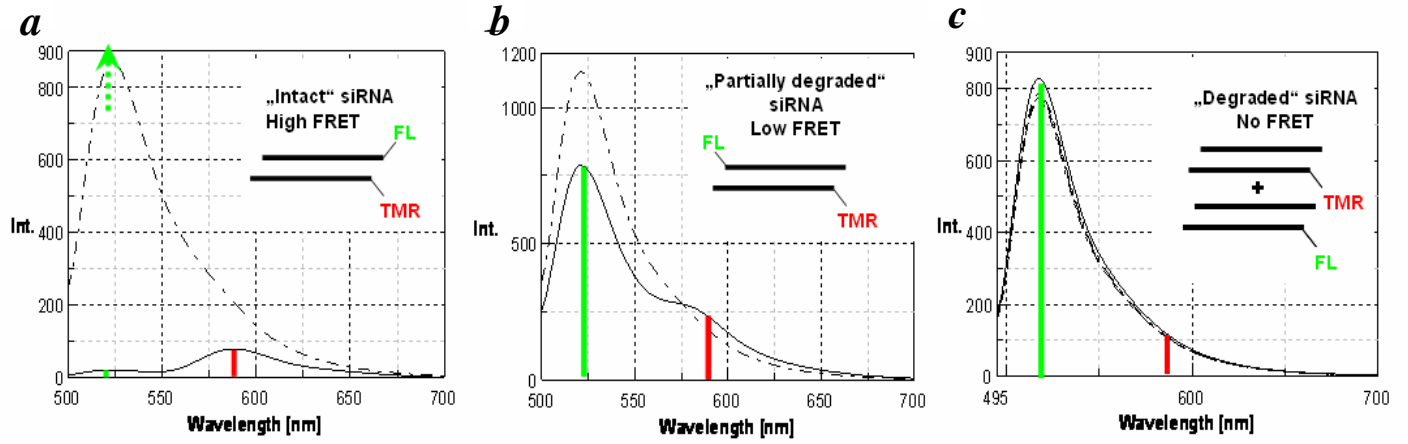


**b**

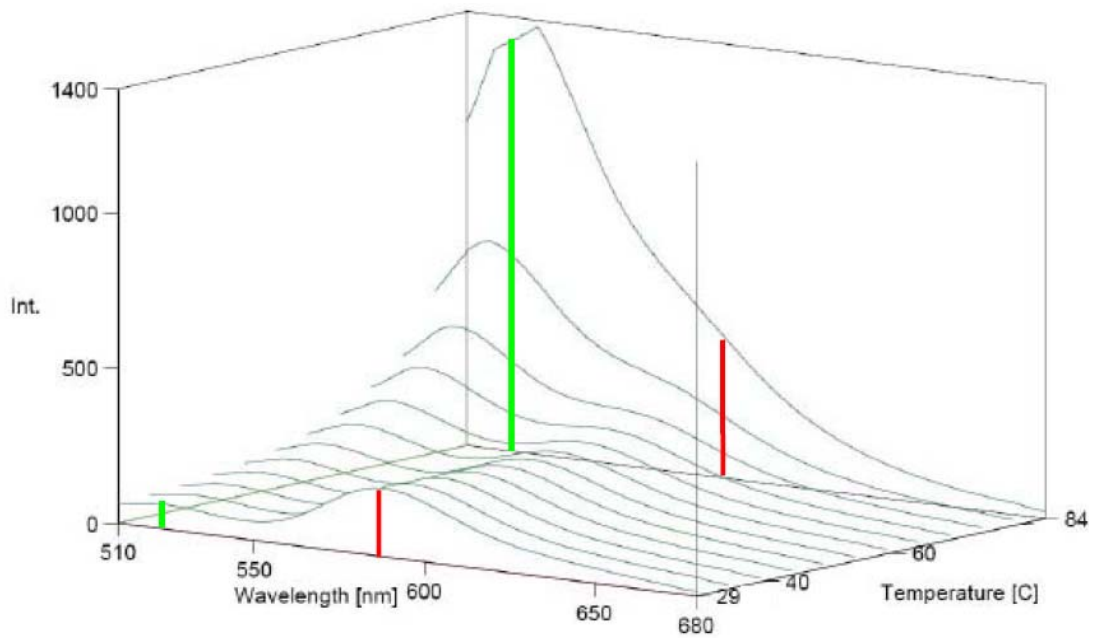


**c**

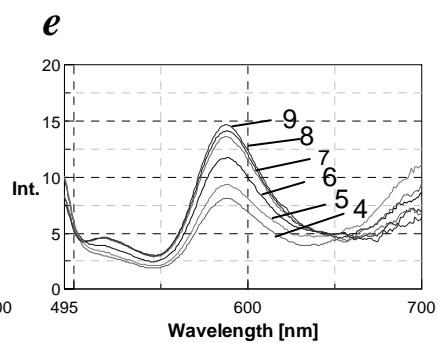
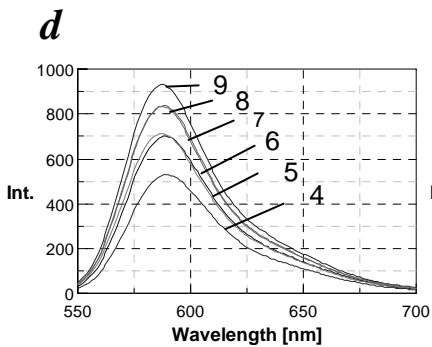
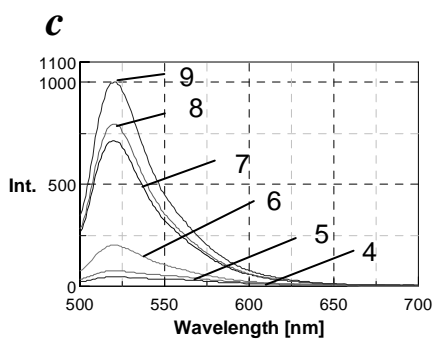
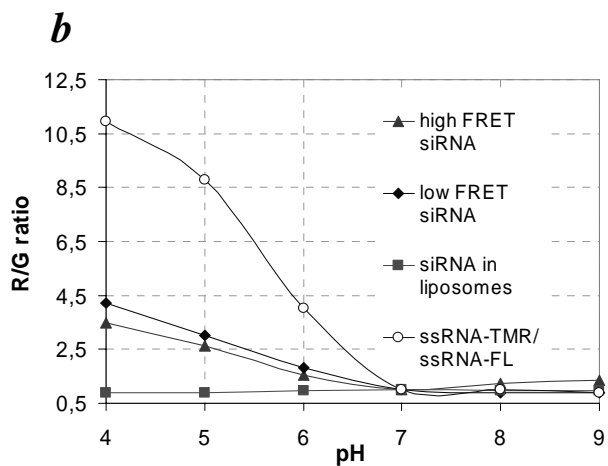
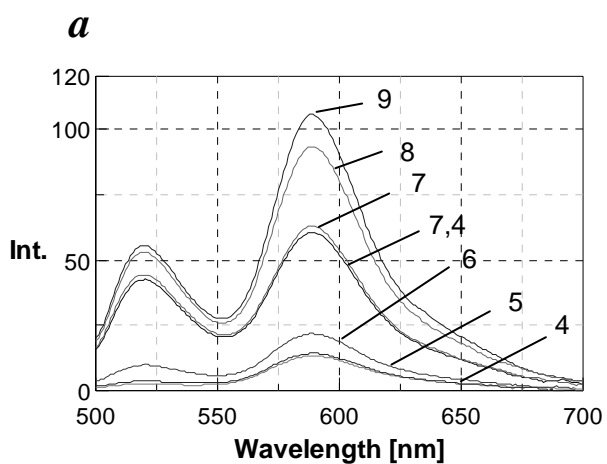




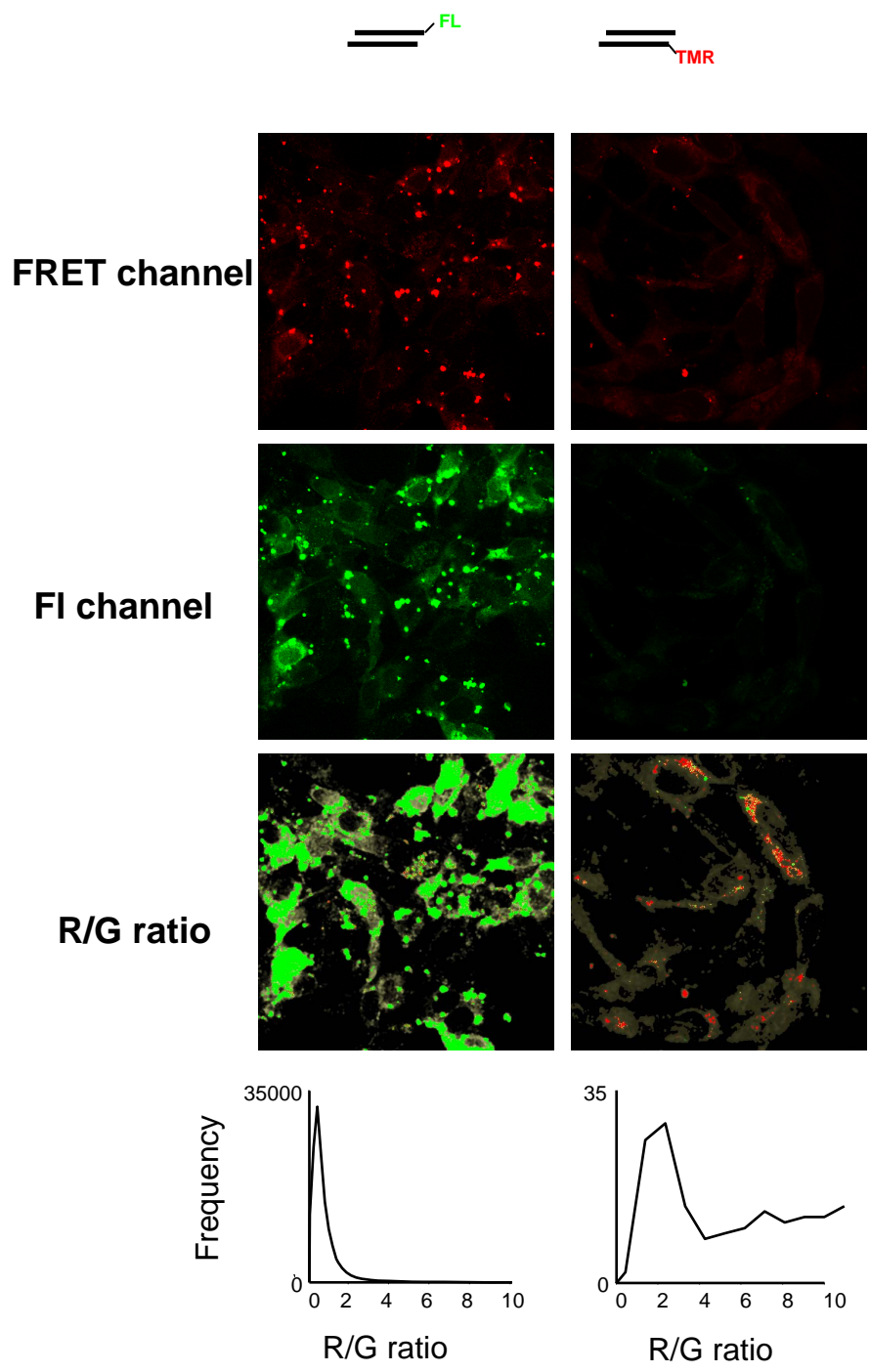
**d**



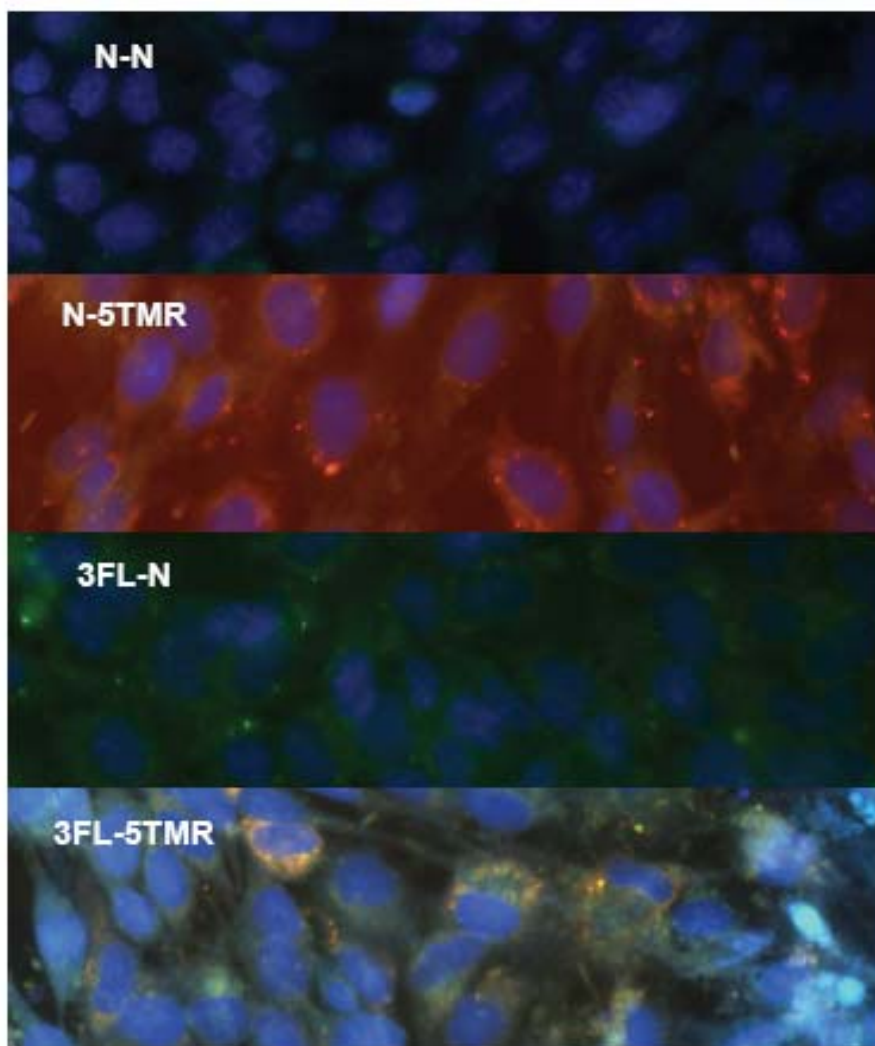
Jaerve *et al* Supplemental Figure S2



Jaerve *et al* Supplemental Figure S3



Jaerve *et al* Supplementary Figure S4



Jaerve *et al* Supplemental Figure S5

## Supplemental material

siRNA	Estimated distance in Å	Estimated $E_{\text{FRET}}$	Experimental $E_{\text{FRET}}$	R/G Ratio [Int <sub>590nm</sub> /Int <sub>520nm</sub> ] before V1 degradation	R/G Ratio [Int <sub>590nm</sub> /Int <sub>520nm</sub> ] after V1 degradation
hiFRET	17	0.97	0.98	>3	0.2
lowFRET	74	0.17	0.18	0.3	0.16
noFRET	>200	0	0	0.13	0.13

### Supplemental Table S1

Properties of dye- labelled siRNAs as model compounds in R/G imaging. The estimated distances and resulting estimated  $E_{\text{FRET}}$  values are based on an A-form RNA helix with 11 base pairs corresponding to a pitch of 30Å per turn, a length of 7,4 Å for the 3'-overhang of two nucleotides, and a linker length for the dye spacer of ~ 9-10 Å.

## Legends to Supplemental Figures

### Supplemental Figure S1

Formula of RNA-conjugated dyes.

(A) TMR-conjugation to 5' or 3' of siRNA, respectively (R=5'-oligo or 3'-oligo)

(B) Fluorescein conjugation to 5' or 3' of siRNA, respectively (R=5'-oligo or 3'-oligo)

(C) Fluorescein conjugation to 3'-of siRNAs *via* linker conjugation to N4 of terminal deoxycytidine.

### Supplemental Figure S2: FRET efficiencies in labelled siRNAs

Emission spectra of “intact”, high-FRET siRNA (A), “partially degraded” low-FRET siRNA (B), and “degraded” no-FRET siRNA (C) upon excitation at 488 nm before (solid line) and after (dashed lines) complete digestion with RNase V1. Emission wavelengths used to calculate FRET efficiencies and R/G ratios are indicated by red and green bars, respectively, and the obtained values are displayed in (D). Melting profile (E): emission spectra of hi-FRET siRNA as a function of temperature.

**Supplementary Figure S3: Dependence of fluorescence spectra on pH variations.**

(A) Emission spectra upon excitation at 488 nm of hi-FRET siRNA at different pH values in PBS.

(B) Evolution of R/G ratio as a function of pH. Solid triangles: hi-FRET siRNA; solid diamonds: lo-FRET siRNA; solid squares: hi-FRET siRNA in liposomes; open circles: ratio of red and green fluorescence of non-complementary single stranded RNAs (ssRNAs) labelled with TMR (excitation at 543 nm) and fluorescein, respectively. The R/G ratios are normalized to values at pH 7.

(C) Emission spectra of fluorescein-labelled ssRNA

(D) Emission spectra of TMR-labelled ssRNA (excitation at 543 nm)

(E) Emission spectra of hi-FRET siRNA in liposomes

**Supplementary Figure S4: R/G imaging of single-labelled siRNAs.** FRET channel, green channel, and R/G imaging of cells 48-72 h post transfection. Histograms of R/G statistics are shown below the R/G images. Note that cells transfected with TMR-only labelled siRNA show very weak fluorescence because excitation of TMR at 488 nm wavelength is very weak (right). Cells transfected with fluorescein-only labelled siRNA (left) shows intense and almost exclusively green voxels in. Pixels identified as belonging to the cell by fluorescence thresholding are in grey in the R/G image.

**Supplementary Figure S5: siRNA are located outside the nucleus one day post transfection.**

RBE4 cells transfected with unlabeled siRNA (N-N; top), antisense 5'-TMR labelled siRNA (N-5TMR; second from the top), sense-3'-fluorescein labelled (3FL-N; second from bottom) and hi-FRET labelled (3FL-5TMR; bottom) siRNA. Cells were fixed, stained with DAPI and scanned in a fluorescence microscope 24 hours post transfection.